PERGAMON

Available online at www.sciencedirect.com
SCIENCE DIRECT®

Polyhedron 22 (2003) 1507–1513

POLYHEDRON
www.elsevier.com/locate/poly

Optically active sulfur-bridged Co(III)–M(II) (M = Pd, Pt) dinuclear complexes with square-planar [M(μ-S)$_2$(bpy)] (bpy = 2,2′-bipyridine) frameworks derived from octahedral bidentate sulfur-donating Co(III) metalloligands

Yasunori Yamada [a,*], Mamoru Uchida [b], Mitsuharu Fujita [b], Yoshitaro Miyashita [b], Ken-ichi Okamoto [b]

[a] *Department of Chemistry and Applied Chemistry, Faculty of Science and Engineering, Saga University, 1 Honjo-machi, Saga, Saga 840-8502, Japan*
[b] *Department of Chemistry, University of Tsukuba, 1-1-1 Tennodai, Tsukuba, Ibaraki 305-8571, Japan*

Received 9 December 2002; accepted 25 February 2003

Abstract

The reactions of the optically active octahedral mononuclear complex, *trans*(*N*)-[Co(D-pen)$_2$]$^-$ (D-pen = D-penicillaminate), with [PdCl$_2$(bpy)] (bpy = 2,2′-bipyridine) and [PtCl$_2$(bpy)] stereoselectively gave the S-bridged dinuclear complexes, [Pd(bpy){Co(D-pen)$_2$}]$^+$ (**1a**) and [Pt(bpy){Co(D-pen)$_2$}]$^+$ (**1b**), respectively. A similar optically active S-bridged dinuclear complex, Δ-[Pt(bpy){Co(aet)$_2$(*R*-pn)}]$^{3+}$ (**2b**; aet = 2-aminoethanethiolate, pn = 1,2-propanediamine), was also obtained by the substitution reaction of $\Delta\Delta$-[Ni{Co(aet)$_2$(*R*-pn)}$_2$]$^{4+}$ with [PtCl$_2$(bpy)]. The crystal structures of **1a**, **1b**, and **2b** were determined by X-ray crystallography, and compared with that of the previously reported Δ-[Pd(bpy){Co(aet)$_2$(*R*-pn)}]$^{3+}$ (**2a**). The Co(III) equatorial planes and the PdN$_2$S$_2$ or PtN$_2$S$_2$ square planes in the **1a** and **1b** are almost coplanar, while those in **2a** and **2b** are somewhat bent from each other. In addition, the distortions from the square planes to tetrahedrons in **2a** and **2b** are more pronounced than those in **1a** and **1b**. Furthermore, all of the bridging S atoms in **1a** and **1b** are stereoselectively unified to the *S* configuration, in contrast to those in **2a** and **2b** with the *R* configuration. These reflect the differences of the optically active Co(III) units in these complexes. The electronic absorption, CD, and ^{13}C NMR spectral behaviors of these complexes are also discussed in relation to their crystal structures.

Keywords: Optically active sulfur-bridged complexes; Dinuclear Co(III)–Pd(II) and Co(III)–Pt(II) complexes; 2,2′-Bipyridine complexes; Crystal structures; Spectrochemistry

---

1. Introduction

Recently, we have found that the central Ni^{2+} ion in the optically active S-bridged trinuclear complex, $\Delta\Delta$-[Ni{Co(aet)$_2$(*R*-pn)}$_2$]$^{4+}$ (aet = 2-aminoethanethiolate, pn = 1,2-propanediamine), which is obtained by the reaction of [Ni(aet)$_2$] with [CoCl$_2$(*R*-pn)$_2$]$^+$, can be substituted by other metal ions [1–3]. In the reaction of $\Delta\Delta$-[Ni{Co(aet)$_2$(*R*-pn)}$_2$]$^{4+}$ with [PdCl$_4$]$^{2-}$, for instance, the Ni^{2+} ion is readily replaced by the Pd^{2+} ion to yield $\Delta\Delta$-[Pd{Co(aet)$_2$(*R*-pn)}$_2$]$^{4+}$, retaining the absolute configurations of the octahedral Co(III) units [2]. This implies that the terminal Δ-*cis*(*S*)-[Co(aet)$_2$(*R*-pn)]$^+$ unit in the complex can be regarded as an optically active metalloligand with two donating S-atoms. A similar function as a bidentate metalloligand is also recognized for the optically active mononuclear complex, *trans*(*N*)-[Co(D-pen)$_2$]$^-$ (D-pen = D-penicillaminate) [4–6]. The use of these octahedral Co(III) units is expected to make possible the stereoselective constructions of various types of S-bridged polynuclear structures, and to give information about the aggregations of optically active S-donating metalloligands around a wide variety of metal centers. Therefore, the

---

* Corresponding author. Tel./fax: +81-952-28-8806.
E-mail address: yyamada@cc.saga-u.ac.jp (Y. Yamada).

0277-5387/03/$ - see front matter © 2003 Elsevier Science Ltd. All rights reserved.
doi:10.1016/S0277-5387(03)00267-5

detailed inquiries into functions as metalloligands and reactivity toward various metal ions should be required for the above two complexes, $\Delta\Delta$-[Ni{Co(aet)$_2$(R-pn)}$_2$]$^{4+}$ and $trans(N)$-[Co(D-pen)$_2$]$^-$, because of their fundamental and theoretical importance. On the other hand, previous works also indicate that some metal ions can be incorporated into optically active S-bridged polynuclear structures with the aid of these complexes, and that the two S atoms in the Δ-$cis(S)$-[Co(aet)$_2$(R-pn)]$^+$ unit and $trans(N)$-[Co(D-pen)$_2$]$^-$ make bridges with the R and S configurations, respectively [1–6]. Furthermore, the directionality of the lone pairs of two S atoms in $trans(N)$-[Co(D-pen)$_2$]$^-$ is sterically restricted compared with the Δ-$cis(S)$-[Co(aet)$_2$(R-pn)]$^+$ unit due to the nature of the ligands [1–6]. Taking into account these facts, it is expected that the two metalloligands incorporate the same metal species in the different coordination manners, depending on the directionality of the lone pairs and/or chirality of the two bridging S atoms. However, there are no examples for the incorporation of the same metal species into S-bridged polynuclear structures involving each of the $trans(N)$-[Co(D-pen)$_2$]$^-$ and Δ-$cis(S)$-[Co(aet)$_2$(R-pn)]$^+$ units. As has been recognized for the polynuclear complexes derived from some types of S-donating metalloligands, the reactions with the square-planar [MX$_2$(bpy)]-type (M = Pd^{II} or Pt^{II}, X = Cl$^-$ or NO$_3$$^-$, bpy = 2,2′-bipyridine) complexes, in which two X ligands are susceptible to substitution by other ligands, can provide variable information on the functions and reactivity of the S-donating metalloligands [2,7–11]. It seems profitable therefore that the S-bridged polynuclear complexes derived from the reactions of [MCl$_2$(bpy)] with $trans(N)$-[Co(D-pen)$_2$]$^-$ and Δ-$cis(S)$-[Co(aet)$_2$(R-pn)]$^+$ units are examined to clarify the natures of these two metalloligands. In the present work, we have investigated the reactions of [MCl$_2$(bpy)] (M = Pd^{II}, Pt^{II}) with $trans(N)$-[Co(D-pen)$_2$]$^-$ and $\Delta\Delta$-[Ni{Co(aet)$_2$(R-pn)}$_2$]$^{4+}$. Spectrochemical properties of the obtained optically active S-bridged dinuclear complexes, [M(bpy){Co{D-pen}$_2$}$_2$]$^+$ (M = Pd (**1a**) and Pt (**1b**)) and Δ-[{M(bpy)}{Co(aet)$_2$(R-pn)}]$^{3+}$ (M = Pd (**2a**) and Pt (**2b**)), among which those of **2a** were already described elsewhere, are discussed in relation to their crystal structures.

2. Experimental

2.1. Materials

K$_2$PtCl$_4$ and Na$_2$PdCl$_4$ were purchased from Tanaka Rare Metal Industries Ltd. D-penicillamine was obtained from Tokyo Chemical Co., Ltd, and 2,2′-bipyridine and CoCl$_2$·6H$_2$O were from Wako Pure Chemical Ind. Co., Ltd K[Co(D-pen)$_2$]·2.5H$_2$O, [PdCl$_2$(bpy)] and [PtCl$_2$(bpy)] were prepared by modified methods from the literature [12–14]. The optically pure precursor compound, $\Delta\Delta$-[Ni{Co(aet)$_2$(R-pn)}$_2$](ClO$_4$)$_4$·H$_2$O, was derived from the reaction of [Ni(aet)$_2$] with cis-[CoCl$_2$(R-pn)$_2$]Cl, which can be obtained by the use of optically resolved R-pn ligands [1]. The complex, Δ-[Pd(bpy){Co(aet)$_2$(R-pn)}](ClO$_4$)$_3$ (**2a**), was prepared by the previously reported procedure [2], using $\Delta\Delta$-[Ni{Co(aet)$_2$(R-pn)}$_2$](ClO$_4$)$_4$·H$_2$O and [PdCl$_2$(bpy)]. The other chemicals were obtained from Wako Pure Chemical Ind. Co., Ltd, or Tokyo Chemical Co., Ltd. All of the chemicals were of reagent grade and used without further purification.

Caution! Perchlorate salts are potentially dangerous explosives. Care must be exercised in handling these perchlorate salts and only small quantities should be used to avoid any untoward incident.

2.2. Preparation of the complexes

2.2.1. Synthesis of [Pd(bpy){Co(D-pen)$_2$}]Cl·3H$_2$O (**1a**Cl·3H$_2$O)

To a brown solution containing K[Co(D-pen)$_2$]·2.5H$_2$O (0.22 g, 0.5 mmol) in 25 ml H$_2$O was added [PdCl$_2$(bpy)] (0.17 g, 0.5 mmol). After the mixture was stirred at 55 °C for 1 h, a saturated NaCl solution (5 ml) was added to the resulting brown solution. The whole was allowed to stand at 25 °C for several days and the resulting brown crystals were collected by filtration. Yield: 0.23 g (65% based on Co). *Anal*. Found: C, 34.10; H, 4.63; N, 7.84%. Calc. for C$_{20}$H$_{32}$N$_4$O$_7$ClS$_2$CoPd (**1a**Cl·3H$_2$O): C, 34.05; H, 4.60; N, 7.94%. UV–Vis spectrum in H$_2$O [ν_{max}, 10^3 cm^{-1} (log ε, mol^{-1} dm^3 cm^{-1})]: 15.82 (1.91), 19.1 (2.1)$^{shoulder\ (sh)}$, 22.7 (2.8)^{sh}, 29.28 (3.82), 31.2 (4.2)^{sh}, 32.31 (4.22), 34.96 (4.22), 42.28 (4.62), 48.3 (4.6)^{sh}. CD spectrum in H$_2$O [ν_{max}, 10^3 cm^{-1} ($\Delta\varepsilon$)]: 15.11 (−5.42), 19.53 (+10.42), 22.9 (−10.1)^{sh}, 25.58 (−16.80), 28.17 (−20.27), 32.36 (+48.94), 35.5 (+36.1)^{sh}, 40.2 (+29.5)^{sh}, 43.29 (+47.69).

2.2.2. Synthesis of [Pt(bpy){Co(D-pen)$_2$}]Cl·3H$_2$O (**1b**Cl·3H$_2$O)

To a brown solution containing K[Co(D-pen)$_2$]·2.5H$_2$O (0.22 g, 0.5 mmol) in 25 ml H$_2$O was added [PtCl$_2$(bpy)] (0.21 g, 0.5 mmol). After the mixture was stirred at 55 °C for 1 h, a saturated NaCl solution (5 ml) was added to the resulting brown solution. The whole was allowed to stand at 25 °C for several days and the resulting brown crystals were collected by filtration. Yield: 0.27 g (68% based on Co). *Anal*. Found: C, 30.28; H, 4.07; N, 6.98%. Calc. for C$_{20}$H$_{32}$N$_4$O$_7$ClS$_2$CoPt (**1b**Cl·3H$_2$O): C, 30.25; H, 4.06; N, 7.06%. UV–Vis spectrum in H$_2$O [ν_{max}, 10^3 cm^{-1} (log ε, mol^{-1} dm^3 cm^{-1})]: 16.25 (2.13), 19.46 (2.16), 25.2 (3.2)^{sh}, 28.6 (3.8)^{sh}, 31.20 (4.28), 32.36 (4.26), 37.2 (4.2)^{sh}, 41.41 (4.43), 49.38 (4.61). CD spectrum in H$_2$O [ν_{max}, 10^3

cm^{-1} ($\Delta\varepsilon$)]: 16.08 (-6.67), 19.53 ($+7.94$), 23.6 (-0.8)^{sh}, 25.51 (-5.66), 28.1 ($+9.6$)^{sh}, 29.2 ($+13.9$)^{sh}, 30.77 ($+16.06$), 38.02 ($+24.82$), 44.84 ($+35.42$).

2.2.3. Synthesis of *Δ-[Pt(bpy){Co(aet)$_2$(R-pn)}](ClO$_4$)$_3$ (**2b**(ClO$_4$)$_3$)*

To a reddish brown solution containing *ΔΔ*-[Ni{Co(aet)$_2$(*R*-pn)}$_2$](ClO$_4$)$_4$·H$_2$O (0.26 g, 0.25 mmol) in 50 ml H_2O was added [PtCl$_2$(bpy)] (0.21 g, 0.5 mmol). After the mixture was stirred at 55 °C for 1 h, a saturated NaClO$_4$ solution (10 ml) was added to the resulting dark red solution. The whole was allowed to stand at 4 °C for several days and the resulting dark red crystals were collected by filtration. Yield: 0.37 g (79% based on Co). *Anal*. Found: C, 21.90; H, 3.23; N, 9.85%. Calc. for **2b**(ClO$_4$)$_3$ = $C_{17}H_{30}N_6O_{12}S_2Cl_3CoPt$: C, 21.84; H, 3.23; N, 9.99%. UV–Vis spectrum in H_2O [ν_{max}, 10^3 cm^{-1} (log ε/mol^{-1} dm^3 cm^{-1})]: 20.08 (2.57), 25.6 (3.1)^{sh}, 28.2 (3.6)^{sh}, 29.5 (3.8)^{sh}, 31.30 (4.30), 32.52 (4.29), 38.2 (4.3)^{sh}, 41.84 (4.48), 47.5 (4.5)^{sh}. CD spectrum in H_2O [ν_{max}, 10^3 cm^{-1} ($\Delta\varepsilon$)]: 19.46 (-6.14), 25.25 (-6.08), 30.5 ($+10.4$)^{sh}, 34.36 ($+23.08$), 37.0 ($+11.5.8$)^{sh}, 39.5 (-6.4)^{sh}, 41.12 (-9.98), 46.08 (-47.23).

2.3. Measurements

The electronic absorption spectra were recorded with a JASCO Ubest V-560 spectrophotometer and the CD spectra with a JASCO J-600 spectropolarimeter. All of the measurements were carried out in aqueous solutions at room temperature. The ^{13}C NMR spectra were recorded with a Bruker AVANCE-600 NMR spectrometer in D_2O for **1a**Cl·3H$_2$O and **1b**Cl·3H$_2$O, and in a 1:1 mixed solvent of CD_3CN and D_2O for **2b**(ClO$_4$)$_3$, using sodium 4,4-dimethyl-4-silapentane-1-sulfonate (DSS) as an internal reference. The elemental analyses (C, H, N) were performed by the Analysis Center of the University of Tsukuba.

2.4. X-ray structure determination

Single crystals of **1a**Cl·3H$_2$O, **1b**Cl·3H$_2$O, and **2b**(ClO$_4$)$_3$ were used for data collection on a Rigaku RASA-7S four-circle diffractometer with graphite-monochromatized Mo Kα radiation. The unit-cell parameters were determined by a least-square refinement of 25 reflections for **1a**Cl·3H$_2$O, **1b**Cl·3H$_2$O, and **2b**(ClO$_4$)$_3$·($11 < \theta < 15°$). The crystal data and experimental parameters are listed in Table 1. The intensity data were collected by the $\omega - 2\theta$ scan technique, and the intensities were corrected for Lorentz and polarization effect. Empirical absorption correction based on a series of Ψ scans were applied. The independent reflections with $I_0 > 2\sigma(I_0)$ were used for structure determinations. The positions of the Co, Pd, Pt, and other non-H atoms were determined by a direct method. The difference Fourier maps based on these atomic positions revealed some remaining non-hydrogen atoms. The structures were refined by a full-matrix least-squares refinement on *F* of the positional parameters and the anisotropic thermal parameters of the non-hydrogen atoms in **1a**Cl·3H$_2$O, **1b**Cl·3H$_2$O, and **2b**(ClO$_4$)$_3$. The hydrogen atoms on the ligands were fixed by the geometrical and thermal constrains (C–H=N–H – 0.95 Å and $U = 1.3U$ (C, N)). The absolute configurations for **1a**Cl·3H$_2$O and **1b**Cl·3H$_2$O were determined on the basis of the known S configurations of the asymmetric carbon atoms in the D-pen ligands, and these structures were supported by the Flack parameters (0.02(3) for **1a**Cl·3H$_2$O and 0.00(1) for **1b**Cl·3H$_2$O) [15,16]. For **2b**(ClO$_4$)$_3$, on the other hand, when the refinement was carried out using a set of parameters containing the *Δ* configuration of the *cis*(*S*)-[Co(aet)$_2$(*R*-pn)]$^+$ unit, the Flack parameter gives a value of 0.01(1). Furthermore, the asymmetric carbon atom of the pn ligand in the *Δ* configuration shows the *R* configuration, which is expected for the used ligand. It can be therefore assumed that the *cis*(*S*)-[Co(aet)$_2$(*R*-pn)]$^+$ unit in **2b**(ClO$_4$)$_3$ takes the *Δ* configuration. All of the calculations were performed on an Indigo II computer using TEXSAN [17].

3. Results and discussion

3.1. Syntheses

The reaction of the optically active mononuclear complex, *trans*(*N*)-[Co(D-pen)$_2$]$^-$, with [PdCl$_2$(bpy)] stereoselectively gave the S-bridged dinuclear complex, [Pd(bpy){Co(D-pen)$_2$}]$^+$ (**1a**). A similar reaction using [PtCl$_2$(bpy)] instead of [PdCl$_2$(bpy)] resulted in the formation of [Pt(bpy){Co(D-pen)$_2$}]$^+$ (**1b**). Both of the [Co(D-pen)$_2$]$^-$ units in **1a** and **1b** adopt the same *trans*(*N*) geometry as the starting material, and the two Cl atoms bound to each of the Pd and Pt atoms in the starting materials are substituted by the two bridging S atoms from the *trans*(*N*)-[Co(D-pen)$_2$]$^-$ unit to form the [M(μ-S)$_2$(bpy)] (M = Pd (**1a**), Pt (**1b**)) frameworks. These imply that *trans*(*N*)-[Co(D-pen)$_2$]$^-$ functions as an effective optically active metalloligand with two donating S atoms toward the square-planar metal. On the other hand, similar optically active S-bridged dinuclear complexes, *Δ*-[M(bpy){Co(aet)$_2$(*R*-pn)}]$^{3+}$ (M = Pd (**2a**), Pt (**2b**)) were also obtained by the substitution reactions of *ΔΔ*-[Ni{Co(aet)$_2$(*R*-pn)}$_2$]$^{4+}$ with [MCl$_2$(bpy)] [2]. The Co(III) units in **2a** and **2b** retain the *Δ*-*cis*(*S*)-[Co(aet)$_2$(*R*-pn)]$^+$ structures in the parental optically active S-bridged trinuclear complexes. Therefore, the *Δ*-*cis*(*S*)-[Co(aet)$_2$(*R*-pn)]$^+$ unit in *ΔΔ*-[Ni{Co(aet)$_2$(*R*-pn)}$_2$]$^{4+}$ can be regarded as an optically active S-donating metalloligand toward the square-

Table 1
Crystallographic data of [Pd(bpy){Co(D-pen)$_2$}]Cl·3H_2O (**1a**Cl·3H_2O), [Pt(bpy){Co(D-pen)$_2$}]Cl·3H_2O (**1b**Cl·3H_2O), and Δ-[Pt(bpy){Co(aet)$_2$(R-pn)}](ClO$_4$)$_3$ (**2b**(ClO$_4$)$_3$)

	1aCl·3H_2O	**1b**Cl·3H_2O	**2b**(ClO$_4$)$_3$
Formula	$C_{20}H_{32}N_4O_7S_2ClCoPd$	$C_{20}H_{32}N_4O_7S_2ClCoPt$	$C_{17}H_{30}N_6O_{12}S_2C_{l3}CoPt$
Formula weight	705.40	794.09	934.96
Crystal dimenions (mm)	0.40 × 0.40 × 0.40	0.20 × 0.20 × 0.55	0.45 × 0.50 × 0.70
Space group	$P6_2$	$P6_2$	$P2_12_12_1$
a (Å)	14.450(2)	14.4769(8)	14.109(3)
b (Å)			16.945(3)
c (Å)	11.814(3)	11.808(1)	12.886(2)
V (Å^3)	2136.4(8)	2143.1(3)	3080(1)
Z	3	3	4
D_{calc} (g cm^{-3})	1.645	1.846	2.016
μ (cm^{-1})	14.98	57.35	55.16
Transmission factor	0.90–1.00	0.84–1.00	0.42–1.00
Scan type	$\omega-2\theta$	$\omega-2\theta$	$\omega-2\theta$
2θ Range (°)	55.1	55.0	55.0
No. of reflections measured	2069	2063	4212
No. of reflections used	1581	1552	3307
No. of variables used	168	168	379
R (R_w)	0.028 (0.045)	0.029 (0.039)	0.037 (0.045)
Goodness-of-fit on F^2	1.33	1.13	1.07
Flack parameter	0.02(3)	0.00(1)	0.01(1)

planar metal, as in the case of *trans*(N)-[Co(D-pen)$_2$]$^-$. The two S atoms in the *trans*(N)-[Co(D-pen)$_2$]$^-$ unit of **1a** and **1b** are stereoselectively unified to the S configurations, while those in the Δ-*cis*(S)-[Co(aet)$_2$(R-pn)]$^+$ unit of **2a** and **2b** make bridges with the R configurations. Furthermore, the directionalities of the lone pairs of the two S atoms in *trans*(N)-[Co(D-pen)$_2$]$^-$ and those in the Δ-*cis*(S)-[Co(aet)$_2$(R-pn)]$^+$ units are considerably distinct from each other based on the natures of the ligands. As a result, these two optically active S-donating metalloligands incorporate the same metal species into the polynuclear structures by intrinsically different coordination manners.

3.2. Crystal structures

An X-ray structural analysis for each of **1a**Cl·3H_2O and **1b**Cl·3H_2O revealed the presence of a discrete monovalent complex cation, one chloride anion, and three water molecules. On the other hand, **2b**(ClO$_4$)$_3$ consists of a discrete trivalent complex cation and three perchlorate anions, as in the case of **2a**(ClO$_4$)$_3$ [2]. Perspective drawings of the complex cations **1a** and **2b** are given in Figs. 1 and 2, respectively, and their selected bond distances and angles are listed in Table 2. As shown in Fig. 1, **1a** contains one Co atom and one Pd atom to form a dinuclear structure. The Co atom in **1a** is surrounded by two N, O, and S atoms from two D-pen ligands, retaining the *trans*(N) geometry of [Co(D-pen)$_2$]$^-$ as in the starting material. Namely, the equatorial coordination sites of the Co atom are occupied by two O and S atoms, and the axial ones by two N atoms to adopt an octahedral *trans*(N)-[Co(D-pen)$_2$]$^-$ unit. The Pd atom in **1a** is coordinated by two N atoms from bpy and two S atoms from the *trans*(N)-[Co(D-pen)$_2$]$^-$ unit, taking a square-planar geometry. The Co(III) equatorial plane and PdS$_2$N$_2$ plane in **1a** are almost coplanar (dihedral angle: 0.32°), and the coplanarity of these planes is more pronounced than that in the previously reported **2a** with the dihedral angle of 5.7° [2]. While the Pd atom in **1a** takes an almost square-planar geometry (dihedral angle between the PdN$_3$N$_4$ and PdSS* planes: 1.4°), the PdN$_2$S$_2$ sphere in **2a** is

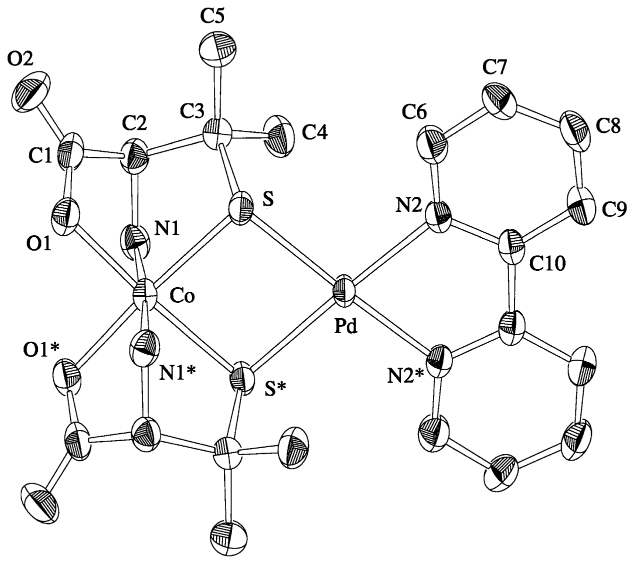

Fig. 1. Perspective view of [Pd(bpy){Co(D-pen)$_2$}]$^+$ (**1a**) with the atomic labelling scheme.

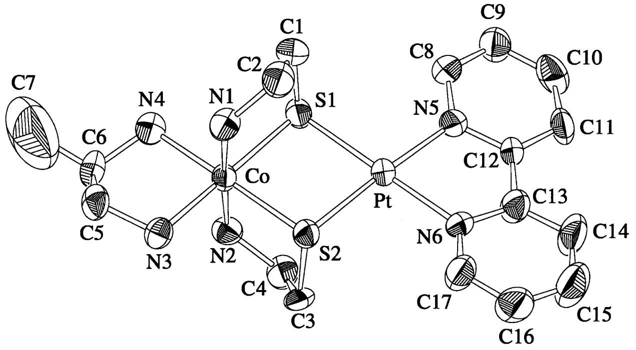

Fig. 2. Perspective view of Δ-$[Pt(bpy)\{Co(aet)_2(R\text{-}pn)\}]^{3+}$ (**2b**) with

Table 2
Selected bond distances (Å) and angles (°) of $[Pd(bpy)\{Co(\textsc{d}\text{-}pen)_2\}]^+$ (**1a**),$[Pt(bpy)\{Co(\textsc{d}\text{-}pen)_2\}]^+$ (**1b**) and Δ-$[Pt(bpy)\{Co(aet)_2(R\text{-}pn)\}]^{3+}$ (**2b**)

M = Pd (**1a**), Pt (**1b**)	M = Pt (**2b**)	**1a**	**1b**	**2b**
Bond distances				
M–S	(M–S1)	2.295(1)	2.299(2)	2.282(2)
M–S*	(M–S2)	2.295(1)	2.299(2)	2.289(2)
M–N2	(M–N5)	2.052(4)	2.036(5)	2.031(8)
M–N2*	(M–N6)	2.052(4)	2.036(5)	2.027(7)
Co–S	(Co–S1)	2.221(1)	2.220(2)	2.244(3)
Co–S*	(Co–S2)	2.221(1)	2.220(2)	2.242(3)
Co–O1	(Co–N4)	1.931(4)	1.931(5)	2.014(8)
Co–O1*	(Co–N3)	1.931(4)	1.931(5)	1.999(7)
Co–N1	(Co–N1)	1.956(4)	1.949(6)	1.982(8)
Co–N*	(Co–N2)	1.956(4)	1.949(6)	1.988(7)
S–C3	(S1–C1)	1.873(5)	1.871(7)	1.80(1)
	(S2–C3)	–	–	1.84(1)
Bond angles				
S–M–S*	(S1–M–S2)	83.57(6)	83.33(7)	82.97(8)
S–M–N2	(S1–M–N5)	98.5(1)	98.6(2)	98.8(2)
S–M–N2*	(S1–M–N6)	177.7(1)	178.1(2)	178.3(2)
S*–M–N2	(S2–M–N5)	177.7(1)	178.1(2)	175.6(2)
S*–M–N2*	(S2–M–N6)	98.5(1)	98.6(2)	98.2(2)
N2–M–N2*	(N5–M–N6)	79.4(2)	79.5(3)	80.0(3)
S–Co–S*	(S1–Co–S2)	87.01(6)	86.99(9)	84.90(9)
S–Co–O1	(S1–Co–N4)	89.5(1)	89.7(1)	95.2(2)
S–Co–O1*	(S1–Co–N3)	175.7(1)	176.0(2)	177.7(2)
S–Co–N1	(S1–Co–N1)	88.2(1)	87.9(2)	88.3(3)
S–Co–N1*	(S1–Co–N2)	95.5(1)	95.9(2)	90.1(2)
S*–Co–O1	(S2–Co–N4)	175.7(1)	176.0(2)	178.0(2)
S*–Co–O1*	(S2–Co–N3)	89.5(1)	89.7(1)	94.3(2)
S*–Co–N1	(S2–Co–N1)	95.5(1)	95.9(2)	90.3(2)
S*–Co–N1*	(S2–Co–N2)	88.2(1)	87.9(2)	87.8(2)
O1–Co–O1*	(N4–Co–N3)	94.1(2)	93.8(3)	85.7(3)
O1–Co–N1	(N4–Co–N1)	82.0(2)	81.9(2)	91.7(3)
O1–Co–N1*	(N4–Co–N2)	94.6(2)	94.5(2)	90.3(3)
O1*–Co–N1	(N3–Co–N1)	94.6(2)	94.5(2)	89.5(3)
O1*–Co–N1*	(N3–Co–N2)	82.0(2)	81.9(2)	92.0(3)
N1–Co–N1*	(N1–Co–N2)	175.0(2)	174.7(4)	177.6(3)
M–S–Co	(M–S1–Co)	94.71(4)	94.84(6)	96.06(10)
(M–S2–Co)	–	–	95.94(9)	
M–S–C3	(M–S1–C1)	111.1(1)	111.7(2)	104.0(4)
(M–S2–C3)	–	–	102.1(3)	
Co–S–C3	(Co–S1–C1)	96.8(1)	96.8(2)	96.8(4)
(Co–S2–C3)	–	–	96.3(3)	

somewhat distorted to a tetrahedral geometry (dihedral angle between the PdN_5N_6 and PdS_1S_2 planes: 4.5°). It can be regarded therefore that the square-planar geometry around the Pd atom in **1a** is less distorted than that in **2a**. Although two chiral configurations, *R* and *S*, are possible for each of the two bridging S atoms in **1a**, both S atoms are stereoselectively unified to the S configuration, consistent with the case of *trans*(*N*)-$[Co(\textsc{d}\text{-}pen)_2]^-$ unit in $[Pd\{Co(aet)_2(en)\}\{Co(\textsc{d}\text{-}pen)_2\}]^{2+}$ [4].

The complex cation **1b** consists of one Co atom and one Pt atom to form a similar dinuclear structure to **1a**, (Fig. 1). As in the case of the Pd atom in **1a**, the Pt atom in **1b** is coordinated by the bidentate bpy ligand and is bridged by two S atoms from the *trans*(*N*)-$[Co(\textsc{d}\text{-}pen)_2]^-$ unit. The Co(III) equatorial plane and PtS_2N_2 plane in **1b** are almost coplanar (dihedral angle: 0.23°), and the extent of the coplanarity is slightly larger than that in **1a**. The dihedral angle between the PtN_3N_4 and PtSS* planes is 0.69°, indicating that the PtN_2S_2 sphere in **1b** is less distorted than the PdN_2S_2 one in **1a**. The bond distances and angles around the Co and Pt atoms in **1b** are almost identical with the corresponding distances and angles in **1a**, except for the Pt–N distances (av. 2.036(5) Å), which are slightly shorter than the Pd–N distances (2.052(4) Å) in **1a** (Table 2). This can be interpreted as an effect of the lanthanide contraction for the Pt atom and/or a result of the stronger affinity with the S atoms of the Pt atom compared to the Pd atom. Similarly to the case of **1a**, on the other hand, both of the two bridging S atoms in **1b** are stereoselectively fixed to the S configuration. It seems therefore that these bridging manners of the S atoms are characteristic for the S-bridged polynuclear structures composed by the *trans*(*N*)-$[Co(\textsc{d}\text{-}pen)_2]^-$ units.

As shown in Fig. 2, the dinuclear structure of **2b**, which is comprised of one Co atom and one Pt atom, is essentially consistent with that of **2a**, except for the difference of the square-planar metal [2]. Namely, **2b** retains the Δ-*cis*(*S*)-$[Co(aet)_2(R\text{-}pn)]^+$ unit in the parental $\Delta\Delta$-$[Ni\{Co(aet)_2(R\text{-}pn)\}_2]^{4+}$ [1]. The *cis*(*S*)-$[Co(aet)_2(R\text{-}pn)]^+$ unit in **2b** adopts the Δ configuration, and the two bridging S atoms are stereoselectively unified to the *R* configurations, in contrast to those in **1b** with *S* configuration. In addition, all of the two aet and one *R*-pn chelate rings in the Δ-*cis*(*S*)-$[Co(aet)_2(R\text{-}pn)]^+$ unit take λ conformations, being attributed by the methyl group of the *R*-pn ligand with equatorial configuration [18]. On the other hand, the non-centrosymmetric space group, $P2_12_12_1$, for $\mathbf{2b}(ClO_4)_3$ indicates that the methyl group of the *R*-pn ligand diminishes the symmetry of the complex from C_2 to C_1 (Table 1). This is a marked contrast to the C_2-symmetrical $[Ni\{Co(aet)_2(en)\}_2]^{4+}$ (en = ethylenediamine), which crystallized in the space group of $C2/c$ [11]. Although the bond distances and angles related to the Pt atom are similar to those in **1b**, the Pt–S–C angles (av. 103.1(4)°) in **2b** are considerably acute compared with the corresponding angle (111.7(2)°) in **1b**. However, the Pt–S–Co and Co–S–C angles in **1b** and **2b** are almost indistinguishable with each other. It can be regarded therefore that the differences in the Pt–S–C angles between **1b** and **2b** are attributable to the octahedral Co(III) units, and that the directionality of lone pairs of the two bridging S atoms in the *trans*(*N*)-$[Co(D\text{-}pen)_2]^-$ and Δ-*cis*(*S*)-$[Co(aet)_2(R\text{-}pn)]^+$ units are significantly distinct from each other. These are also reflected by the facts that the co-planarity between the Co(III) equatorial plane and PtN_2S_2 square plane in **1b** is different from that in **2b** (dihedral angle: 5.3°), and that the PtN_2S_2 square plane in **1b** is less distorted than that in **2b** (dihedral angle between the PdN_2 and PdS_2 planes: 4.1°).

3.3. Characterization

As shown in Table 3, each ^{13}C NMR spectrum of **1a** and **1b** shows five signals due to the D-pen ligands and five signals characteristic for the bpy ligand in D_2O [10,11]. Among the five signals due to the D-pen ligands, δ 30.92 and 34.55 for **1a** are assigned to the carbon atoms of $-CH_3$ groups in the D-pen ligands [4–6]. The remaining three signals due to D-pen ligands at 55.88, 75.42, and 183.59 for **1a** are ascribed to the carbon atoms of $-C(CH_3)_2S$, $-CH(COO)N$, and $-COO$ groups, respectively. Although ten carbon atoms of one bpy and two D-pen ligands are present in each of **1a** and **1b**, no other peaks were found in the ^{13}C NMR spectra of these complexes. Furthermore, all the signals due to the bpy and D-pen ligands in **1b** are identical with those in **1a**, but are slightly shifted compared with those in **1a**, reflecting the difference of the involving d^8 metal ions. It seems therefore that two pyridyl moieties of one bpy ligand and two D-pen ligands in each of **1a** and **1b** are almost equivalent to each other, and that the complexes retain their symmetrical S-bridged dinuclear structures in solution as in the solid state (Fig. 1). On the other hand, **2b** exhibits seven signals due to the $[Co(aet)_2(R\text{-}pn)]^+$ unit and five signals due to the bpy ligand in a 1:1 mixed solvent of CD_3CN and D_2O. Among the seven signals due to the $[Co(aet)_2(R\text{-}pn)]^+$ unit, the signals at 37.13 and 37.25 are ascribed to the $-CH_2S$ groups in the aet ligands [1–3]. Furthermore, the signals due to the $-CH_2N$ groups in the aet ligands also appear as two signals at 52.24 and 53.68. These facts indicate that the two aet ligands are not equivalent to each other, as in the case of the corresponding Pd complex, **2a** [2]. On the other hand, the two pyridyl moieties of the bpy ligand in **2b** are almost equivalent to each other, and therefore observed as five signals. All the signals in **2b** are slightly shifted compared with the corresponding signals in **2a**, indicating the influence of the d^8 metal ions. Since no other peaks were found in the spectrum of **2b** for periods exceeding one week, the complex is relatively stable in solution and retains the S-bridged dinuclear structure, which is expected to be almost the same as that in the crystalline state.

Table 3
^{13}C NMR chemical shifts [a] of $[Pd(bpy)\{Co(D\text{-}pen)_2\}]^+$ (**1a**) and $[Pt(bpy)\{Co(D\text{-}pen)_2\}]^+$ (**1b**) in D_2O, and of Δ-$[Pt(bpy)\{Co(aet)_2(R\text{-}pn)\}]^{3+}$ (**2b**) in a 1:1 mixed solvent of CD_3CN and D_2O

	1a	1b	2b
$-CH_3$ (D-pen)	30.92	31.01	–
	34.55	34.61	–
$-C(CH_3)_2S$ (D-pen)	55.88	54.91	–
$-CH(COO)N$ (D-pen)	75.42	75.81	–
$-COO$ (D-pen)w	183.59	183.49	–
$-CH_2S$ (aet)	–	–	37.13
	–	–	37.25
$-CH_2N$ (aet)	–	–	52.24
	–	–	53.68
$-CH_3$ (*R*-pn)	–	–	19.35
$-CH_2N$ (*R*-pn)	–	–	56.25
$-CHN$ (*R*-pn)	–	–	57.19
Carbon atoms in bpy	126.83	127.10	126.96
	130.76	131.24	131.18
	144.72	144.91	144.86
	151.34	150.15	149.26
	158.99	159.33	158.56

[a] In ppm from DSS.

Electronic absorption and CD spectra of **1a**, **1b,** and **2b** in H_2O are shown in Fig. 3. The first absorption band of **1a** is comprised of three components at 15.82, 19.1, and 22.7×10^3 cm^{-1}. In addition, **1a** shows a second d–d and sulfur-to-metal charge-transfer bands at 29.28 and 34.96×10^3 cm^{-1}, respectively [6,12]. Furthermore, the characteristic bands due to the localized electronic transitions on the bpy framework appear at 31.2 and 32.31×10^3 cm^{-1} [2,9,11]. Although a similar absorption spectral pattern is also observed for **1b**, all the bands concerning the Co(III) center are significantly shifted compared with the corresponding bands of **1a**. This implies that the metal species in the {M(bpy)} moieties considerably affect the electronic nature of the dinuclear complexes. On the other hand, **2b** shows two d–d bands due to the Co^{3+} ion at 20.08 and 25.6×10^3 cm^{-1}, two S-to-Co CT bands at 38.2 and 41.84×10^3 cm^{-1}, and two localized electronic bands on bpy at 31.30 and 32.52×10^3 cm^{-1}. Among these bands, the 31.30 and 32.52×10^3 cm^{-1} bands are located at the slightly higher-energy-side compared with the corresponding bands (31.20 and 32.36×10^3 cm^{-1}) of **1b**. This indicates that the electronic states of the bpy frameworks in these complexes are influenced by the Co(III) units through the S-bridged Pt(II) atoms. The remaining three intense bands at 28.2, 29.5 and 47.5×10^3 cm^{-1} seem to be related to the Pt^{2+} ion, since the

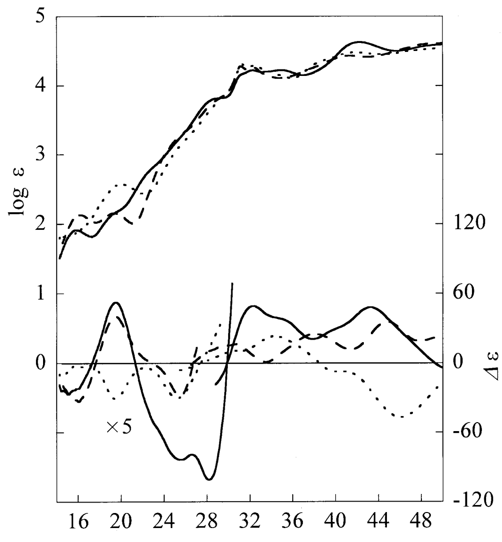

Fig. 3. Electronic absorption and CD spectra of $[Pd(bpy)\{Co(\text{D-pen})_2\}]^+$ (**1a**) (—), $[Pt(bpy)\{Co(\text{D-pen})_2\}]^+$ (**1b**) (---), and Δ-$[Pt(bpy)\{Co(aet)_2(R\text{-pn})\}]^{3+}$ (**2b**) (·····) in H_2O.

corresponding bands are also observed for $\Delta\Delta$-$[Pt\{Co(aet)_2(R\text{-pn})_2\}]^{4+}$ [3]. The CD spectral behaviors of **1a** and **1b** are similar to each other, but are considerably different from that of *trans*(*N*)-$[Co(\text{D-pen})_2]^-$ over the whole region except for the first absorption band region [6,12]. This reflects the formation of the $[M(\mu\text{-}S)_2(bpy)]$ frameworks in **1a** and **1b** with the S-donating bidentate metalloligand, *trans*(*N*)-$[Co(\text{D-pen})_2]^-$. Although the CD spectra of **1a** and **1b** correspond well with each other, the behaviors around 28×10^3 cm^{-1} are significantly different from each other. Namely, **1a** shows an intense negative CD band at 28.17×10^3 cm^{-1}, while **1b** shows a weak shoulder with positive CD sign at 28.1×10^3 cm^{-1}. Furthermore, the intensities of the lower-energy-side two bands (22.9 and 25.58×10^3 cm^{-1}) in **1a** are appreciably larger than those of the corresponding bands (23.6 and 25.51×10^3 cm^{-1}) in **1b**. These imply that the CD spectra in the region are largely dependent on the d^8 metal species in the dinuclear complexes. On the other hand, the CD spectral behavior of **2b** corresponds well with that of **2a** over the whole region. While the CD spectra of the Pt(II) complexes, **1b** and **2b**, are almost symmetric, both complexes show the negative CD bands around 25×10^3 cm^{-1} with almost the same intensities as each other. Such CD spectral behaviors are not observed for the Pd complexes, **1a** and **2a**, the spectra of the two complexes are almost symmetric over the whole region. Therefore, it can be concluded at least that the Pt(II) atoms considerably contribute to the CD spectra of **1b** and **2b** in this region.

4. Supplementary material

Crystallographic data for the structural analysis have been deposited with the Cambridge Crystallographic Data Centre, CCDC Nos. 198397, 198398, and 198399 for **1a**$Cl\cdot 3H_2O$, **1b**$Cl\cdot 3H_2O$, and **2b**$(ClO_4)_3$, respectively. Copies of this information may be obtained free of charge from The Director, CCDC, 12 Union Road, Cambridge CB2 1EZ, UK (fax: +44-1223-336033; e-mail: deposit@ccdc.cam.ac.uk or www: http://www.ccdc.cam.ac.uk).

Acknowledgements

This work was partially supported by a Grant-in-Aid for Scientific Research No. 14540510 from the Ministry of Education, Science, Sports, and Culture.

References

[1] Y. Yamada, Y. Maeda, Y. Miyashita, K. Fujisawa, T. Konno, K. Okamoto, Bull. Chem. Soc. Jpn 73 (2000) 1219.
[2] Y. Yamada, Y. Maeda, T. Konno, K. Fujisawa, K. Okamoto, Bull. Chem. Soc. Jpn 73 (2000) 1831.
[3] Y. Yamada, Y. Miyashita, K. Fujisawa, K. Okamoto, Bull. Chem. Soc. Jpn 75 (2002) 1151.
[4] T. Konno, N. Matsuno, K. Okamoto, M. Hirotsu, Chem. Lett. (1999) 1243.
[5] T. Konno, M. Hattori, T. Yoshimura, M. Hirotsu, Chem. Lett. (2000) 852.
[6] Y. Yamada, M. Tsumita, A. Hirano, Y. Miyashita, K. Fujisawa, K. Okamoto, Inorg. Chim. Acta 332 (2002) 108.
[7] T. Konno, Y. Yoshinari, K. Okamoto, Chem. Lett. (1995) 989.
[8] K. Okamoto, Y. Yoshinari, Y. Yamada, N. Sakagami, T. Konno, Bull. Chem. Soc. Jpn 1363 (1998) 71.
[9] Y. Yamada, K. Okamoto, Chem. Lett. (1999) 315.
[10] Y. Yamada, M. Uchida, Y. Miyashita, K. Fujisawa, T. Konno, K. Okamoto, Bull. Chem. Soc. Jpn. 73 (2000) 913.
[11] Y. Yamada, K. Fujisawa, K. Okamoto, Bull. Chem. Soc. Jpn 73 (2000) 2067.
[12] K. Okamoto, K. Wakayama, H. Einaga, S. Yamada, J. Hidaka, Bull. Chem. Soc. Jpn 56 (1983) 165.
[13] N. Baidya, D. Ndreu, M. Olmstead, K. Mascharak, Inorg. Chem. 30 (1991) 2448.
[14] R.H. Herber, M. Croft, M.J. Coyer, B. Bilash, A. Sahiner, Inorg. Chem. 33 (1994) 2422.
[15] H.D. Flack, Acta Crystallogr., Sect. A 39 (1983) 876.
[16] H.D. Flack, G. Bernandinello, Acta Crystallogr., Sect. A 41 (1985) 500.
[17] TEXSAN. Molecular Structure Corporation. Single Crystal Structure Analysis Software, version 1.9, MSC, 3200 Research Forest Drive, The Woodlands, TX 77381, USA, 1998.
[18] E.J. Corey, J.C. Bailar, Jr., J. Am. Chem. Soc. 81 (1959) 2620.